ECS Journal of Solid State Science and Technology, 2020 **9** 016015

Broad Green Emission in the Leucite-Like $Cs_2ZnSi_5O_{12}$:Eu^{2+} Phosphor

Shruti Hariyani, * **Edward Armijo,** and **Jakoah Brgoch** **,z

Department of Chemistry, University of Houston, Houston, Texas 77204, USA

Cesium zinc silicate substituted with Eu^{2+} has been synthesized as a new green-emitting phosphor with potential application in UV-based solid state white lighting. $Cs_2ZnSi_5O_{12}$ has been known to exhibit polymorphism, crystallizing in space group *Pbca* as well as $Pa\bar{3}$, as a structural analog to the cubic leucite, $CsAlSi_2O_6$. Using laboratory X-ray powder diffraction and optical spectroscopy, the crystal structure of $Cs_2ZnSi_5O_{12}$:Eu^{2+}, when prepared using high-temperature ceramic synthesis, was confirmed to adopt space group $Pa\bar{3}$. This novel phosphor produces a broad green emission ($\lambda_{em} = 504$ nm) upon UV excitation. Encapsulating the compound in optically transparent silicone resin along with the red-emitting $Sr_2Si_5N_8$:Eu^{2+} and exciting with a UV-LED ($\lambda_{ex} = 370$ nm) produces a warm white light with excellent color rendering. The advantage of developing a light using $Cs_2ZnSi_5O_{12}$:Eu^{2+} is that the broad green emission negates the need for incorporating three different phosphors as is commonly required for UV-pumping. This dramatically simplifies device design while still achieving high-quality UV-based white light. Once the emission efficiency and thermal stability of $Cs_2ZnSi_5O_{12}$:Eu^{2+} is improved, there can be seamless integration with UV-LEDs for high-quality warm white light production.

 [DOI: 10.1149/2.0222001JSS]

Manuscript submitted July 30, 2019; revised manuscript received October 7, 2019. Published October 29, 2019. *This paper is part of the JSS Focus Issue on Recent Advances in Wide Bandgap III-Nitride Devices and Solid State Lighting: A Tribute to Isamu Akasaki.*

The outstanding operating lifetimes, high efficiencies, and environmentally benign components have made solid state lighting the preferred choice for replacing traditional fluorescent and incandescent based light bulbs.[1,2] Considering the global need for the reduction of electricity consumption, the shift toward LED lighting is opportune.[3] These devices produce a functional white light through the combination of an inorganic phosphor and an LED chip, where the phosphor down-converts the LED's emission to longer wavelengths. The most common method of white lighting production uses a blue-emitting (InGa)N LED coated with a yellow-emitting phosphor, such as cerium substituted yttrium aluminum garnet.[4] This method generates cheap, functional lighting but has the drawback of producing a cool, blue-tinted white light with a high correlated color temperature (CCT) and low color rendering index (CRI). To support the transition from conventional lighting sources, cost-effective warmer white lights with lower CCTs and higher values of CRI are needed. One method capable of alleviating the high CCT and low CRI is through the addition of a second, red-emitting phosphor such as $Sr_2Si_5N_8$:Eu,[2] $SrAlSiN_3$:Eu^{2+}, or K_2SiF_6:Mn^{4+}.[5] This solution is the current industrial approach and is capable of producing highly efficient warm white lights; however, these lights still miss photons in the 400 nm to 450 nm region that are vital for high-value lighting. A second solution is combining three inorganic phosphors (blue, red, and green-emitting materials) with a UV-LED. This method can also produce a warm white light with the added advantages of color selectivity and tunability, depending on the ratio of the three phosphors, as well as covering the near-UV region. The caveat with this approach is that all three phosphors must be highly efficient due to the inherent Stokes' loss in emission intensity as a by-product of the conversion process.[3,6] Thus, further advancing solid state lighting requires not only the continued improvement to the LED chips but also the development of new inorganic phosphors.

Inorganic phosphors typically consist of a host lattice that has a rare-earth ion, i.e., Ce^{3+} or Eu^{2+}, substituted onto the cation site. The incorporation of the rare-earth ion induces crystal field splitting where the *5d* orbitals of the activator ion experience a downward shift, allowing the $4f \leftrightarrow 5d$ electronic transitions to occur within the visible region of the electromagnetic spectrum.[7] The crystal chemistry of the phosphor is critical to understanding the efficiency of this down-conversion process, the position of the excitation and emission wavelength, the width of the emission band, and the thermal properties. Some of the most widely-used and studied red and blue-emitting phosphors are $Sr_2Si_5N_8$:Eu^{2+}, $Sr_{1-x}Ca_xAlSiN_3$:Eu^{2+}, K_2SiF_6:Mn^{4+} and $BaMgAl_{10}O_{17}$:Eu^{2+}, $Na_3Sc_2(PO_4)_3$:Eu^{2+}, $RbBaPO_4$:Eu^{2+}, among others.[8–12] These phosphors possess photoluminescent quantum yields (PLQY) approaching 100%, satisfactory thermal stability, and scalable synthetic routes. There are also many other red and blue-emitting phosphors that are reported in the literature that provide an array of possible luminescent materials for application.[13,14] The current obstacle in the creation of high-quality white lighting is, therefore, the development of new green-emitting phosphors. Green phosphors are comparatively rare with only a handful of these compounds reported. The industry standard green-emitting phosphor is β-SiAlON:Eu^{2+} owing to its narrow, bright green emission; however, this phase requires extreme synthetic conditions including reacting at temperatures of ≈1950°C in a pressurized environment, followed by washing with HF to obtain a pure phase product.[15] β-SiAlON:Eu^{2+} is regularly used for display lighting, cerium substituted lutetium aluminum garnet ($Lu_{3-x}Ce_xAl_5O_{12}$) is more often used as a green-emitter for general illumination purposes. However, this phosphor suffers from poor near-UV (<400 nm) excitation necessary for pc-LEDs.[16]

Orthosilicates are a popular alternative due to the low cost of precursor oxides and ease of synthesis.[17] Substituting compounds following the general formula M_2SiO_4 (M = Ba, Ca, Sr) with Eu^{2+} typically results in phosphors that emit in the 500 nm to 600 nm range upon excitation from 300 nm to 400 nm.[5] One of the most popular of these compositions is the green-emitting Ba_2SiO_4:Eu^{2+}, which has a PLQY of 75%. A drawback of this material is that Ba_2SiO_4:Eu^{2+} loses half of its initial emission intensity upon heating at 150°C. This can be resolved by forming a solid solution with both Sr^{2+} and Ca^{2+}, which has been known to enhance color tunability and thermal stability.[5] Further, this particular family of silicates crystallizes in relatively low symmetry structures, *Pmcn* for Ba_2SiO_4 and $P2_1/n$ for both Ca and Sr_2SiO_4, resulting in broad emission bands and moderate quantum yields.[18] Past research has indicated that the discovery of host structures should instead be highly symmetric, rigid crystal structures to overcome these limitations.[19–24] Therefore, in the search for novel host structures, we turn to highly symmetric, densely packed silicates as potential phosphors.

One type of silicate that is of particular interest is based on the mineral leucite ($A_2{}^+B^{2+}Si_5O_{12}$), which exists as various polymorphs depending on composition and synthetic conditions.[25] These leucite-like silicates are known to crystallize with a variety of permutations where A^+ = Na, K, Rb, Cs and B^{2+} = Mg, Fe^{2+}, Co, Zn, Cd, Mn.[25–28] Although these compound can incorporate an array of elements, un-

*Electrochemical Society Student Member.
**Electrochemical Society Member.
zE-mail: jbrgoch@uh.edu

derstanding their crystal chemistry remains difficult. For example, silicates like $K_2B^{2+}Si_5O_{12}$ (B^{2+} = Fe^{2+}, Co, Zn) can transition between the monoclinic $P2_1/c$ and cubic $Ia\bar{3}$ d, whereas some compositions exhibit no structural changes, such as $Cs_2B^{2+}Si_5O_{12}$ (B^{2+} = Cd, Cu).[25,26] Interestingly, the only $Cs_2B^{2+}Si_5O_{12}$ silicate that has been reported to exhibit polymorphism in the orthorhombic *Pbca* and cubic $Pa\bar{3}$ is $Cs_2ZnSi_5O_{12}$. However, a $Cs_2MgSi_5O_{12}$:Eu^{2+} phosphor, which seems to be isostructural to $Cs_2ZnSi_5O_{12}$, has been reported to luminesce green upon UV excitation and possess robust thermal stability.[29] These leucite structures are densely packed due to the rigid framework composed of comer-sharing [SiO_4] tetrahedra, making them ideal host structures for potential phosphors. In this work, we prepare a new cubic leucite-like phase, $Cs_2ZnSi_5O_{12}$, obtained using high-temperature solid state synthesis. Substituting Cs in this compound with Eu^{2+}, following $Cs_{2-x}Eu_xZnSi_5O_{12}$, results in an emission centered in the green region of the visible spectrum upon UV excitation. The multiple crystallographically independent Eu^{2+} positions generate a broad emission that spans from 400–700 nm making this phosphor a viable candidate, in combination with a red-emitting phosphor, for creating a UV-based warm white phosphor-converted LED (pc-LED.)

Experimental

Polycrystalline samples of $Cs_2ZnSi_5O_{12}$ (CZSO) and $Cs_{2-x}Eu_xZnSi_5O_{12}$ (x = 0.02, 0.03, 0.04, 0.06, and 0.08) (CZSO:Eu^{2+}) were synthesized by combining the starting powders of Cs_2CO_3 (Alfa Aesar, 99%), ZnO (Alfa Aesar, 99.9%), SiO_2 (Sigma-Aldrich, 99.5%), and Eu_2O_3 (Materion Advanced Chemicals, 99.9%) in the required stoichiometric ratios. After a preliminary mixing in an agate mortar and pestle, the powders were further ground in an acetone medium before being milled in a high-energy ball mill (Spex 8000 M Mixer/Mill) for 30 minutes. The resulting powders were pressed into pellets (6mm) before being placed into an alumina crucible (AdValue Technology) on a bed of sacrificial powder to avoid contamination from the crucible. The powders were fired in a tube furnace for 12 hours at 1000°C under a reducing (5% H_2/95% N_2) environment with heating and cooling rates of 3°C/minute. The resulting powders were ground into a fine powder using an agate mortar and pestle followed by washing with 1M HCl and then dried.

The products obtained from the furnace were ground in an agate mortar and pestle and checked for phase purity using a Cu Kα (1.54183 Å) PanAnalytical powder diffractometer. Refinements were conducted using the EXPGUI interface of GSAS where the background was fit with a shifted Chebyshev function, and the peak shapes were modeled by the pseudo-Voigt function with additional Finger-Cox-Jephcoat asymmetry to correct for axial divergence observed at low angles. The mixed occupancies were fixed as previously reported. The refined crystal structure was visualized using VESTA.

The optical characterization was performed by depositing the polycrystalline products onto a quartz slide (Chemglass) after mixing the powders into a silicone resin (GE Silicones, RTV615). Room temperature and temperature-dependent photoluminescent spectra were obtained employing a Horiba Fluoromax-4 fluorescence spectrophotometer with a 75 W xenon arc lamp for excitation, and a Janis cryostat (VPF-100) for a controlled temperature environment from 80–500 K. The optical bandgap was experimentally determined by diffuse reflectance measured using an Agilent Technologies Cary 5000 with a diffuse reflectance attachment. The internal photoluminescent quantum yield was measured and calculated by applying the method of de Mello et al. and using a Spectralon-coated integrating sphere (150 mm diameter, Labsphere) with an excitation wavelength of 365 nm.[30] Luminescent lifetime was determined using a Horiba DeltaFlex Lifetime System with a NanoLED N-360 nm (λ_{ex} = 363 nm) LED. Fabrication of a pc-LED involved the use of lab-made $Sr_2Si_5N_8$:Eu^{2+} and the $Cs_{1.92}Eu_{0.04}ZnSi_5O_{12}$ and mixing in the same silicone resin mentioned above. The phosphor "cap" was prepared by curing the phosphor resin in a custom brass mold and excited using a 370 nm LED with a 30 mA current. The pc-LED electroluminescence spectrum and performance was characterized using an AvaSpehere-50-IRRAD spectrophotometer and the corresponding AvaSoft 8 software.

Table I. Rietveld refinement data and statistics for $Cs_2ZnSi_5O_{12}$.

Refined formula	$Cs_2ZnSi_5O_{12}$
Radiation type, λ (Å)	1.54183 Å
2θ range (deg)	5–90
Temperature (K)	295
Crystal System	Cubic
Space group; Z	$Pa\bar{3}$; 8
Lattice parameters (Å)	13.6582(1)
Volume(Å^3)	2547.90(1)
R_p	0.0670
R_{wp}	0.0948
X^2	3.070

Results and Discussion

Structure refinement and description.—$Cs_2ZnSi_5O_{12}$ has been reported to exhibit polymorphism crystallizing in orthorhombic space group *Pbca* at room temperature and undergoing a structural transition to cubic space group $Pa\bar{3}$ at 663 K.[25] Both structures are considered leucite analogs due to structural similarities to conventional tetragonal leucites.[25] Tetragonal leucites crystalize in *I*4/*a* and have the composition $A^+AlSi_2O_6$, where A^+ is a group one metal.[31] The structure is composed of four-membered and six-membered rings formed by corner-connected tetrahedra composed of statistically mixed [SiO_4] and [AlO_4], creating a three-dimensional framework.[25] Much like the $Cs_2ZnSi_5O_{12}$ system, the $A^+AlSi_2O_6$ leucite system (A^+ = K, Rb, Cs) has been known to exhibit a phase transformation to cubic, (space group $Ia\bar{3}$ d) upon heating from 93 K to 298 K.[32] In all of these structures, there are condensed [(Si/Al)O_4] rings that generate two voids within the structure, a larger one, filled by the A^+ cation, and a smaller one which remains empty. This structural foundation gives rise to a highly connected crystal structure that can incorporate rare-earth ions, making these phases of significant interest as potential phosphor hosts.

Past research has shown that these leucite-like structures are indeed ideal host structures for potential phosphors. $CsAlSi_2O_6$, a structural analog of the previously mentioned leucite-like structure, crystallizes in $Ia\bar{3}$ d and exhibits a broad blue-green emission upon UV-excitation when substituted with Eu^{2+}, and possesses a PLQY of 67%. Additionally, this phosphor is known to exhibit robust thermal stability by retaining 75% of the room temperature emission upon heating to 425 K.[33] The addition of K, following $Cs_{1-x}K_xAlSi_2O_6$, causes the emission to blue-shift while exhibiting similar thermal stability as the parent compound.[34] A third leucite-like phosphor $Cs_2MgSi_5O_{12}$:Eu^{2+} shows a broad green emission from 400–700 nm that can be deconvoluted into two separate emission peaks at 475 and 550 nm. Similarly to the other leucite-like phosphors, this compound also exhibits enhanced thermal stability.[29] Because of the robust luminescent and thermal properties of these leucite-like phosphors, it is predicted that the $Cs_2ZnSi_5O_{12}$:Eu^{2+} phosphor will also exhibit the same enhanced properties.

The desired products, $Cs_2ZnSi_5O_{12}$ and $Cs_{2-x}Eu_xZnSi_5O_{12}$ (x = 0.02, 0.03, 0.04, 0.06, and 0.08), were therefore prepared by heating the starting powders at 1000°C for 12 hours (Figure S1). The inclusion of Eu^{2+} showed no changes in the host crystal structure, except for the expected changes in lattice parameters (Figure S2). The powder X-ray diffractograms suggested the product could be indexed as either space group $Pa\bar{3}$ or $Ia\bar{3}$ d. However, Rietveld refinement, plotted in Figure 1, confirmed that $Cs_2ZnSi_5O_{12}$ likely adopts the $Pa\bar{3}$ space group. The refinement statistics and refined crystal structure data are provided in Table I and Table II, respectively.

CZSO crystallizes in the cubic $Pa\bar{3}$ structure with a refined lattice parameter of 13.6582(1) Å, creating a massive cubic unit cell with a volume of 2547.90(1) Å^3. The crystal structure, determined by a Ri-

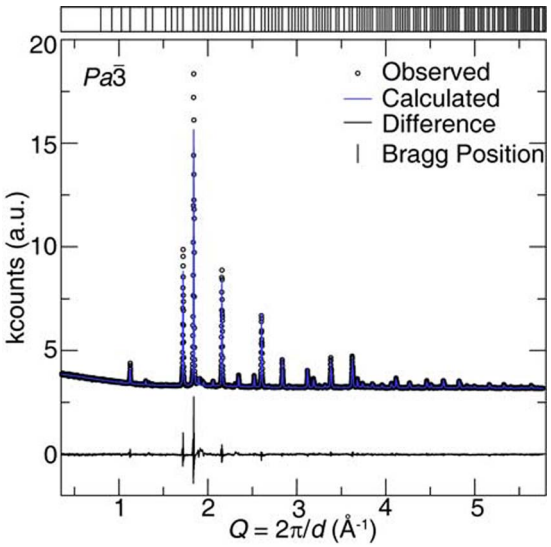

Figure 1. Rietveld refinement of laboratory (Cu Kα) X-ray powder diffraction data indicate $Cs_2ZnSi_5O_{12}$ crystallizes in space group $Pa\bar{3}$.

etveld refinement of the powder X-ray diffraction data, is illustrated in Figure 2. The structure is composed of a framework of Si-centered and Zn/Si-centered polyhedra that are corner connected. The Si(1)–O bond distances in the tetrahedra fall within a range of 1.609 to 1.650 Å while the bond distances of the Zn^{2+} containing polyhedra are slightly larger, ranging between 1.680 to 1.755 Å, owing to the inclusion of the larger Zn^{2+}($r_{4\text{-coord.}}$ = 0.60 Å) as compared to the smaller Si^{4+} ($r_{4\text{-coord.}}$ = 0.26 Å).[35] The resulting small, highly connected polyhedra undoubtedly give rise to a very rigid backbone, forming cavities that are occupied by Cs. The structure contains two independent Cs atoms that are both 12-coordinated with oxygen, with a polyhedral volume of 87.27 Å^3 and 99.69 Å^3. When comparing this polyhedral volume to the *Pbca* polymorph, the values of the polyhedral volume are much larger, 105.51, and 112.53 Å^3, respectively.[36] These larger are volumes are due to the slightly elongated bond lengths, most likely stemming from the lower symmetry. Indeed, when comparing these volumes to the [CsO_{12}] polyhedra in the higher symmetry *I*4/*a* and $Ia\bar{3}$ *d* polymorphs of $CsAlSi_2O_6$, similar polyhedral volumes of 97.15 Å^3 and 96.12 Å^3, respectively, are observed where again volume decreases upon an increase in symmetry.[32]

The presence of two crystallographically independent Cs positions in $Pa\bar{3}$ is critically important to understand this phosphor, especially when compared to the single crystallographically independent Cs present in the $Ia\bar{3}$ *d* structure, as narrow emitting phosphors tend to have only one crystallographic position for the luminescent center. When examining these space groups more closely, it is found that $Pa\bar{3}$ is a subgroup of $Ia\bar{3}$ *d*. Examining the relationship between these space group shows that in $Ia\bar{3}$ *d,* the Cs atoms occupy the single 16*c*

Table II. Refined atomic positions, thermal parameters for $Cs_2ZnSi_5O_{12}$.

Atom	Wyck. Pos.	*x*	*y*	*z*	U_{iso} (Å^2)	occ.
Cs1	8*c*	0.12279	0.12279	0.12279	0.051(2)	1
Cs2	8*c*	0.38428	0.38428	0.38428	0.038(5)	1
Si1	24*d*	0.36551	0.83868	0.91588	0.025(8)	0.333
Zn1	24*d*	0.36551	0.83868	0.91588	0.025(8)	0.666
Si2	24*d*	0.12671	0.65765	0.59150	0.0074(6)	1
O1	24*d*	0.47995	0.40915	0.14733	0.0069(3)	1
O2	24*d*	0.11903	0.72499	0.12926	0.019(9)	1
O3	24*d*	0.96327	0.88663	0.68557	0.038(7)	1
O4	24*d*	0.63508	0.21148	0.61138	0.042(11)	1

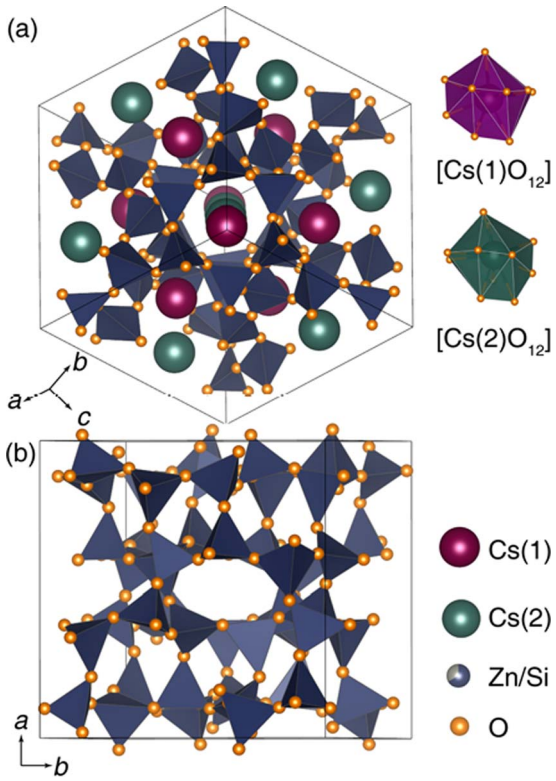

Figure 2. (a) View of $Cs_2ZnSi_5O_{12}$ along the [111] body diagonal. Cs atoms sit in the cavities produced by the silicon tetrahedra. Each Cs atom is coordinated by 12 oxygen atoms. (b) The [SiO_4] and [(Si/Zn)O_4] tetrahedra form four and six-membered rings that make up the rigid framework.

Wyckoff site, leading to one distinct emission site, whereas for $Pa\bar{3}$, the original 16*c* site is split into two 8*c* Wyckoff sites. The result is an expected two independent emission peaks. Additionally, the 48*g* and 96*h* sites that the Al/Si and O atoms occupy are also split into 2 and 4 distinct 24*d* sites, respectively. These lower Wyckoff positions are the results of the loss of body centering and dihedral mirror plane when decreasing in symmetry from $Ia\bar{3}$ *d* to $Pa\bar{3}$. Therefore, a broader emission in $Cs_2ZnSi_5O_{12}$:Eu^{2+} may be expected compared to if this phase adopted the higher symmetry, $Ia\bar{3}$ *d* space group.

Photoluminescent properties.—Substituting Eu^{2+} in CZSO results in a bright green luminescence upon UV (λ_{ex} = 365 nm) excitation. Undoubtedly, the Eu^{2+} ($r_{12\text{-coord.}}$ = 1.48 Å) occupies the much larger Cs^+ ($r_{12\text{- coord.}}$ = 1.88 Å) site despite the isovalency with the much too small Zn^{2+} ($r_{4\text{-coord.}}$ = 0.60 Å).[35] Examining the photoluminescent excitation spectrum (Figure 3a) reveals a broad excitation peak centered at 307 nm and expanding up to 400 nm. For application in a UV-based pc-LED device, UV-A (λ_{ex} = 365 – 400 nm) excitation wavelengths are typically employed. Exciting CZSO:Eu^{2+} at λ_{ex} = 365 nm yields a broad emission peak from 400 nm to 700 nm with the peak centered at λ_{em} = 504 nm. At room temperature, this broad emission has a full width at half maximum of 4139 cm^{-1} (156 nm). The peak can be deconvoluted into two emission peaks that are centered at 500 nm and 580 nm, with an FWHM of 3891.5 cm^{-1} and 2771.2 cm^{-1}, respectively. This further supports the presence of two crystallographically independent Cs(Eu) sites in this structure. Monitoring the excitation spectrum of each emission peak at different emission wavelengths indicates a virtually identical excitation spectrum, suggesting the coordination environments of these luminescent centers are very similar. A small anomaly is also observed in the emission spectrum at $\lambda_{em} \approx$ 611 nm that most likely stems from the presence of a minute amount of Eu^{3+} that was unable to be reduced, even when using 15% H_2/85% N_2 gas during reaction. This impurity is likely a charge compensa-

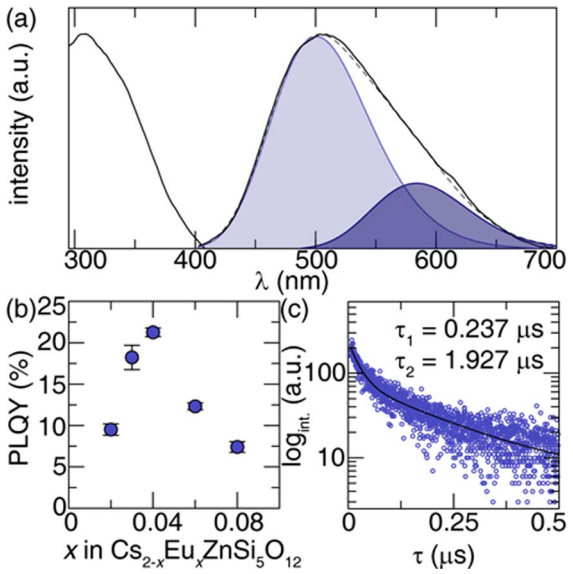

Figure 3. (a) Photoluminescent excitation (λ_{em} = 504 nm) and emission (λ_{ex} = 365 nm) spectrum of $Cs_2ZnSi_5O_{12}$:Eu^{2+}. The emission can be deconvoluted into two peaks at 500 and 580 nm. (b) The optimized concentration of Eu^{2+} was determined as $x = 0.04$, which yields a PLQY of 21.6%. (c) Photoluminescent decay spectrum using 360 nm excitation and monitored at wavelengths >400 nm. The data was fit (black line) according to a bi-exponential function.

tion mechanism from the site substitution of divalent europium for monovalent cesium. Further investigation of the two emission peaks is carried out by analyzing the local structure of the two Cs positions. The [CsO_{12}] polyhedral volume was calculated along with the bond distortion index and the polyhedral quadratic elongation according to Equations 1 and 2, respectively.

$$D = \frac{1}{n}\sum_{i=1}^{n}\frac{|l_i - l_{avg.}|}{l_{avg.}} \quad [1]$$

$$\langle\lambda\rangle = \frac{1}{n}\sum_{i=1}^{n}\left(\frac{l_i}{l_{avg.}}\right)^2 \quad [2]$$

The bond length distortion D, is a function of l_i, the distance between the coordinating *ith* atom and central atoms, and $l_{avg.}$ is the average bond length. The quadratic elongation of polyhedra, <λ>, is calculated similarly in which l_0 is the distance between the central atom and vertex for a regular polyhedron where a quadratic elongation value of 1 indicates a perfect polyhedron. The bond distortion index of Cs(1) was found to be 0.0817 Å with a quadratic elongation of 1.062 Å whereas Cs(2) has a bond distortion index and quadratic elongation of 0.0252 Å and 1.100 Å, respectively. The quadratic elongation values for both Cs(1) and Cs(2) are comparable, but because of the very low value of the bond distortion index for Cs(2), the Cs(2) site is deemed to be a more symmetric environment than the Cs(1) site. Upon substitution, this trend is also observed. Considering a higher degree of symmetry for a luminescent center is known to cause a smaller Stokes' shift, this may inhibit non-radiative relaxation pathways.[22] Thus, the Cs(2) site is predicted to have enhanced luminescent properties compared to the Cs(1) site. However, the difference is small; therefore, any improvement is expected to be negligible. Finally, the calculated polyhedral volume can be used to approximate crystal field splitting to assign each distinct emission to a particular Cs site. The polyhedral volumes of the Cs(1) and Cs(2) site are 87.27 $Å^3$ and 99.69 $Å^3$, respectively. As the Cs(1) site has a distinctly smaller polyhedral volume, the effects of crystal field splitting will be more significant, causing emission to occur at longer wavelengths. Therefore, the emission peak centered at 500 nm can be assigned to the Cs(2) site, whereas the emission at 580 nm is attributed to the Cs(1) site.

To determine the optimal substitution concentration of Eu^{2+}, samples with the compositions $Cs_{2-x}Eu_xZnSi_5O_{12}$ (x = 0.02, 0.03, 0.04, 0.06, and 0.08) were synthesized, and the internal PLQY was measured using an excitation wavelength of 365 nm. As seen in Figure 3b, the room temperature PLQY of the compound was 21.6(5)% when $x = 0.04$. Owing to the high symmetry and rigid nature of this crystal structure, it was predicted that this phosphor would be highly efficient; thus, the lower PLQY was somewhat surprising. To confirm that the low, observed PLQY was not the result of parasitic absorption from residual ZnO remaining in the product, the powders were washed with hydrochloric acid. The luminescence efficiency and powder X-ray diffractogram remained unchanged indicating the low PLQY cannot be attributed to an interfering impurity (Figure S3). However, the significant size difference between the Eu^{2+} and Cs^+ can lead to the presence of soft-phonon modes because the Eu^{2+} can "rattle" upon excitation. Additionally, the aliovalent substitution will generate defects within the crystal structure, including the presence of Eu^{3+} in the product. Together, this generates a substantial number of non-radiative quenching mechanisms that each negatively affect the PLQY. Additionally, due to the presence of two crystallographically independent Cs sites in such a densely packed structure, quenching may also occur due to energy transfer between doping sites. The critical distance of energy transfer (*Rc*) was, therefore calculated to determine the probability of energy transfer. This distance can be calculated using Equation 3 where V is the volume of the unit cell, x_c is the optimized rare-earth concentration and n is the sum of the Wyckoff positions of the crystallographically independent substitution sites.[37]

$$R_c = 2\left(\frac{3V}{4\pi x_c n}\right)^{1/3} \quad [3]$$

The probability of energy transfer between two activator ions is determined by their interatomic distances: should the interatomic distance exceed the value of *Rc*, then it is said that the probability of energy transfer is improbable.[38] Upon further investigation of the refined unit cell, the nearest neighbor Cs(1) – Cs(2) distance was calculated to be only 4.834 Å because of channels that contain the chains of Cs atoms that run along the [111] direction. It is unsurprising that the critical distance is much larger, 13.63 Å, due to the large unit cell volume. Because the Cs(1) – Cs(2) distance is smaller than the critical distance, it is possible that energy transfer is acting as a quenching mechanism and is also causing the observed low PLQY. It is worth noting that this explanation is reliant upon the assumption that all of the rare-earth is fully incorporated into the host. If not, this value of the critical distance may significantly differ. Nevertheless, further optimization through improved synthesis and post-processing techniques, such as additional high temperature annealing steps, must be done before this material can be more readily applied in lighting.[39]

Monitoring the photoluminescent decay of CZSO:Eu^{2+} upon excitation at 363 nm produces a decay curve that can be fitted with a bi-exponential function following Equation 4,

$$I = I_0 + A_1 e^{-t/\tau_1} + A_2 e^{-t/\tau_2} \quad [4]$$

where I is the luminescent intensity, A_1 and A_2 are constants, and τ_1 and τ_2 represent two independent decay times measured as a function of time. These data confirm the presence of two independent substitution sites since the decay occurs via two separate lifetimes, 0.237 μs and 1.927 μs (Figure 3c). The lifetimes are typical of that of Eu^{2+} doped phosphors due to the degeneracy of the excited $4f^6\,5d^1$ states, causing delayed relaxation down to the $4f$ ground state.

Temperature-dependent photoluminescence and device integration.—When developing new phosphors for use in conjunction with LEDs for solid state lighting, the emission stability with respect to temperature must be considered. As pc-LED devices undergo prolonged use in harsh environments, the overall device temperature increases, which will cause an adverse effect on the

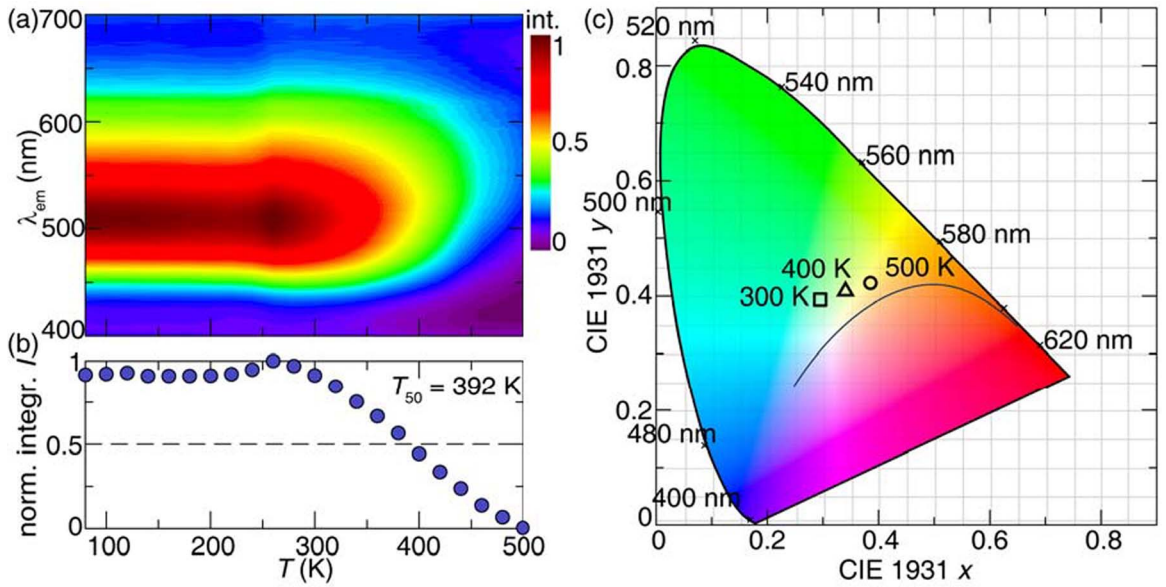

Figure 4. (a) Temperature dependent photoluminescence and (b) the normalized, integrated emission intensity as a function of temperature for $Cs_2ZnSi_5O_{12}:Eu^{2+}$. (c) The room temperature (square), 400 K (triangle) and 500 K (circle) emission was plotted on the 1931 CIE, depicting a redshift upon increasing temperature.

PLQY and color stability of the phosphors. Thus, thermally robust phosphors must be identified prior to adoption in a pc-LED device. To quantify thermal stability, the T_{50}, or temperature at which emission becomes 50% of the room temperature emission, can be determined.[40] Figure 4 shows the normalized, integrated emission intensity of CZSO:Eu^{2+} as a function of temperature from 80–500K. Increasing the temperature from 80 K to 260 K shows a small, but uncharacteristic increase in emission intensity that likely stems from the presence of trap states that arise due to the disparity between rare-earth and substitution site size and their aliovalent substitution. Nevertheless, the emission intensity remains relatively stable up to 360 K; however, increasing the temperature beyond 360 K causes a sharp decline in the emission intensity where at 500 K, the emission is almost entirely quenched. The T_{50} occurs at 392 K, which is considerably less than the operating temperature of most LED lights (423 K). This intense thermal quenching is somewhat surprising considering $CsAlSi_2O_6:Eu^{2+}$, which also crystallizes as a cubic leucite analog, retains 75% of room temperature emission intensity at 425 K.[33] Additionally, the structurally analogous material $Cs_{1.97}Eu_{0.03}MgSi_5O_{12}$ did not show any significant thermal quenching at 423 K.[29] One possible explanation of the observed lack of thermal stability for CZSO:Eu^{2+} compared to the structurally analogous Mg silicate could be due to the presence of a d^{10} Zn^{2+} ion. The presence of this d^{10} ion may be the cause of the narrow experimental bandgap which allows for photoionization, where a photon is further promoted to the conduction band, to more readily occur and thus, the sample emission to be quenched.

The optical bandgap (E_g) can be obtained for the unsubstituted CZSO using diffuse reflectance measurements and converting to absorbance by applying the Kubelka-Munk transformation following Equation 5,

$$(hvF\,(R_\infty))^{1/n} = A\left(hv - E_g\right) \qquad [5]$$

where h is Planck's constant, v is the photon frequency, $F(R_\infty)$ is the measured, corrected absorbance, A is a proportional constant, and n is equal to $\frac{1}{2}$ for this direct bandgap compound. From this approach, an $E_g = 3.12$ eV is obtained. Additionally, diffuse reflectance measurements on the CZSO:Eu^{2+} phosphor were conducted and show a slight decrease in the bandgap to 3.05 eV (Figure S4). The bandgap remains virtutally unchanged after washing the CZSO:Eu^{2+} with 1 M HCl (Figure S3). More importantly, the absorption from the 5*d* orbitals is centered at ≈3 eV, just below the conduction band edge. The proximity of the rare-earth excited state orbitals to the conduction band indicates this phase may undergo photoionization quenching at moderate temperatures. Therefore, the substitution of Zn^{2+} for Mg^{2+} negatively influences the crystal structure's temperate dependent optical properties, but additional research is necessary to understand the exact origin of this change.

In addition to investigating thermal stability with respect to emission intensity, color stability is also taken into account when selecting phosphors for incorporation in pc-LED devices. Color stability is determined by a material's resistance to changes in emission wavelength as a function of temperature.[41] Similar to emission intensity, the emission wavelength remains stable until 320 K, with 1931 CIE coordinates of (0.2954, 0.3936). The emission peak then begins to redshift with increasing temperature, as plotted in Figure 4c. This substantial change in the observed emission is the result of asymmetric quenching between the two emission peaks where the peak centered at 500 nm quenches more rapidly than the peak centered at 580 nm, hence the overall redshift of the emission color (Figure S5).

Finally, CZSO:Eu^{2+} was evaluated for practical use in a pc-LED. CZSO:Eu^{2+} (30 wt%), along with a small amount of $Sr_2Si_5N_8:Eu^{2+}$ (0.1 wt%) for the presence of a red-emitter, was mixed in optically transparent silicon. Figure 5a shows the broad-spectrum white light obtained by exciting the phosphor mixture using a forward bias of 30 mA, with a 370 nm emitting UV LED. This warm, white light using CZSO:Eu^{2+} exhibits a CCT of 3108 K, a CRI R_a value of 90.2, and has CIE coordinates of (0.4362, 0.4154), which is near the Planckian locus, meaning the emission mimics the emission seen from black body radiation. (Figure 5b) This warm-white light is widely sought after in homes and offices.[42] Owing to the broad emission of CZSO:Eu^{2+}, the incorporation of a third blue-emitting phosphor was unnecessary. The ability to still obtain a warm white light with excellent color rendering using a UV-pump with only two phosphors dramatically reduces the cost of potential UV-based LED device fabrication.

Conclusions

In summary, a novel phosphor based on a leucite-like structure belonging to the $Pa\bar{3}$ space group, $Cs_2ZnSi_5O_{12}:Eu^{2+}$ was synthesized. $Cs_2ZnSi_5O_{12}:Eu^{2+}$ is comprised of a rigid framework formed by four and six-membered rings composed of corner connected silicon tetrahedra where half of the tetrahedra are partially occupied by Zn^{2+}. The cubic structure of $Cs_2ZnSi_5O_{12}:Eu^{2+}$ was confirmed by the presence

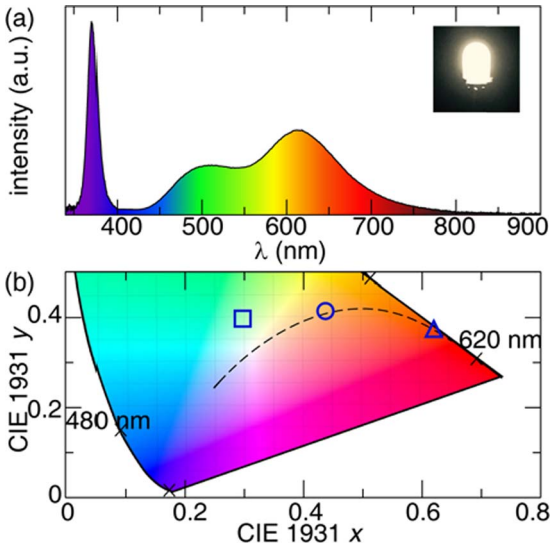

Figure 5. (a) Broad-spectrum white light made from the combination of $Cs_2ZnSi_5O_{12}:Eu^{2+}$ and $Sr_2Si_5N_8:Eu^{2+}$, excited by a 30 mA 365nm-LED. No blue component was needed to achieve a warm, white light. (b) CIE coordinates of the fabricated white light (circle) made from $Cs_2ZnSi_5O_{12}:Eu^{2+}$ (square) and $Sr_2Si_5N_8:Eu^{2+}$(triangle). The dashed line shows the Planckian locus.

of two separate Eu^{2+} emission peaks from two crystallographically independent Cs^+ sites, seen only in the $Pa\bar{3}$ structure. When excited with UV light, CZSO:Eu^{2+} emits bright green, with an extremely broad emission that spans the blue and green portion of the visible region. However, $Cs_2ZnSi_5O_{12}:Eu^{2+}$ suffers from a low PLQY, likely due to the size mismatch between the substitution site and activator ion. Despite this limitation, $Cs_2ZnSi_5O_{12}:Eu^{2+}$ exhibits moderate thermal stability, and the fabrication of a device using this novel phosphor showed that a broad-spectrum warm white light with a high CRI and low CCT could be produced. Therefore, CZSO:Eu^{2+} would be an ideal material for use in pc-LEDs and full-spectrum lighting applications once the emission efficiency and thermal stability is greatly improved.

Acknowledgments

The authors thank the National Science Foundation (DMR 18-47701 and CER 19-11311). This work was also supported by the R. A. Welch Foundation (E-1981) and the State of Texas through the Texas Center for Superconductivity at the University of Houston (TCSUH). The authors are also grateful that Dr. A. Henderson helped us get in contact with Dr. A. Bell, who generously provided the original data from his work on this subject. The authors declare no competing financial interest.

ORCID

Shruti Hariyani https://orcid.org/0000-0002-4707-8863
Edward Armijo https://orcid.org/0000-0001-5242-0806
Jakoah Brgoch https://orcid.org/0000-0002-1406-1352

References

1. H. A. Höppe, "Recent developments in the field of inorganic phosphors." *Angew. Chem. Int. Ed.*, **48**(20), 3572 (2009).
2. J. K. Kim and E. Fred Schubert, "Transcending the replacement paradigm of solid-state lighting." *Opt. Express*, **16**(26), 21835 (2008).
3. X. Qin, X. Liu, W. Huang, M. Bettinelli, and X. Liu, "Lanthanide-activated phosphors based on 4*f*-5*d* optical transitions: Theoretical and experimental aspects." *Chem. Rev.*, **117**(5), 4488 (2017).
4. S. Pimputkar, J. S. Speck, S. P. DenBaars, and S. Nakamura, "Prospects for LED lighting." *Nat. Photonics*, **3**, 180 (2009).
5. N. C. George, K. A. Denault, and R. Seshadri, "Phosphors for solid-state white lighting." *Annu. Rev. Mater. Res.*, **43**(1), 481 (2013).
6. T. Jüstel, H. Nikol, and C. Ronda, "New developments in the field of luminescent materials for lighting and displays." *Angew. Chem. Int. Ed.*, **37**(22), 3084 (1998).
7. S. Ye, F. Xiao, Y. X. Pan, Y. Y. Ma, and Q. Y. Zhang, "Phosphors in phosphor-converted white light-emitting diodes: Recent advances in materials, techniques and properties." *Mater. Sci. Eng., R.* **71**(1), 1 (2010).
8. K.-B. Kim, Y.-I. Kim, H.-G. Chun, T.-Y. Cho, J.-S. Jung, and J.-G. Kang, "Structural and optical properties of $BaMgAl_{10}O_{17}:Eu^{2+}$ phosphor." *Chem. Mater.*, **14**(12), 5045 (2002).
9. H. Watanabe and N. Kijima, "Crystal structure and luminescence properties of $Sr_xCa_{1-x}AlSiN_3:Eu^{2+}$ mixed nitride phosphors." *J. Alloys Compd.*, **475**(1), 434 (2009).
10. H. F. Sijbom, R. Verstraete, J. J. Joos, D. Poelman, and P. F. Smet, "$K_2SiF_6:Mn^{4+}$ as a red phosphor for displays and warm-white LEDs: a review of properties and perspectives." *Opt. Mater. Express*, **7**(9), 3332 (2017).
11. Y. H. Kim, P. Arunkumar, B. Y. Kim, S. Unithrattil, E. Kim, S.-H. Moon, J. Y. Hyun, K. H. Kim, D. Lee, J.-S. Lee, and W. B. Im, "A zero-thermal-quenching phosphor." *Nat. Mater.*, **16**, 543 (2017).
12. H. J. Song, D. K. Yim, H.-S. Roh, I. S. Cho, S.-J. Kim, Y.-H. Jin, H.-W. Shim, D.-W. Kim, and K. S. Hong, "$RbBaPO_4:Eu^{2+}$: a new alternative blue-emitting phosphor for UV-based white light-emitting diodes." *J. Mater. Chem. C*, **1**(3), 500 (2013).
13. S. Ye, F. Xiao, Y. X. Pan, Y. Y. Ma, and Q. Y. Zhang, "Phosphors in phosphor-converted white light-emitting diodes: Recent advances in materials, techniques and properties." *Mater. Sci. Eng., R*, **71**(1), 1 (2010).
14. R.-J. Xie and N. Hirosaki, "Silicon-based oxynitride and nitride phosphors for white LEDs—A review." *Sci. Technol. Adv. Mater.*, **8**(7–8), 588 (2007).
15. J. Brgoch, M. W. Gaultois, M. Balasubramanian, K. Page, B.-C. Hong, and R. Seshadri, "Local structure and structural rigidity of the green phosphor β-SiAlON:Eu^{2+}." *Appl. Phys. Lett.*, **105**(18), 181904 (2014).
16. K. Park, T. Kim, Y. Yu, K. Seo, and J. Kim, "Y/Gd-free yellow $Lu_3Al_5O_{12}:Ce^{3+}$ phosphor for white LEDs." *J. Lumin.*, **173**, 159 (2016).
17. J. Brgoch, C. K. H. Borg, K. A. Denault, A. Mikhailovsky, S. P. DenBaars, and R. Seshadri, "An efficient, thermally stable cerium-based silicate phosphor for solid state white lighting." *Inorg. Chem.*, **52**(14), 8010 (2013).
18. Y. Sato, H. Kato, M. Kobayashi, T. Masaki, D.-H. Yoon, and M. Kakihana, "Tailoring of deep-red luminescence in $Ca_2SiO_4:Eu^{2+}$." *Angew. Chem. Int. Ed.*, **53**(30), 7756 (2014).
19. K. A. Denault, J. Brgoch, S. D. Kloß, M. W. Gaultois, J. Siewenie, K. Page, and R. Seshadri, "Average and local structure, Debye temperature, and structural sigidity in some oxide compounds related to phosphor hosts." *ACS Appl. Mater. Interfaces*, **7**(13), 7264 (2015).
20. P. Pust, V. Weiler, C. Hecht, A. Tücks, A. S. Wochnik, A.-K. Henß, D. Wiechert, C. Scheu, P. J. Schmidt, and W. Schnick, "Narrow-band red-emitting $Sr[LiAl_3N_4]:Eu^{2+}$ as a next-generation LED-phosphor material." *Nat. Mater.*, **13**, 891 (2014).
21. L. Chen, C.-C. Lin, C.-W. Yeh, and R.-S. Liu, "Light converting inorganic phosphors for white light-emitting diodes." *Materials*, **3**(3), 2172 (2010).
22. A. C. Duke, S. Hariyani, and J. Brgoch, "$Ba_3Y_2B_6O_{15}:Ce^{3+}$—A high symmetry, narrow-emitting blue phosphor for wide-gamut white lighting." *Chem. Mater.*, **30**(8), 2668 (2018).
23. G. J. Dirksen and G. Blasse, "Luminescence in the pentaborate $LiBa_2B_5O_{10}$." *J. Solid State Chem.*, **92**(2), 591 (1991).
24. N. C. George, A. J. Pell, G. Dantelle, K. Page, A. Llobet, M. Balasubramanian, G. Pintacuda, B. F. Chmelka, and R. Seshadri, "Local environments of dilute activator ions in the solid-state lighting phosphor $Y_{3-x}Ce_xAl_5O_{12}$." *Chem. Mater.*, **25**(20), 3979 (2013).
25. A. M. T. Bell and C. M. B. Henderson, "High-temperature synchrotron X-ray powder diffraction study of $Cs_2XSi_5O_{12}$ (X = Cd, Cu, Zn) leucites." *Miner. Mag*, **76**(5), 1257 (2012).
26. A. M. T. Bell and C. M. B Henderson, "Crystal structures of $K_2[XSi_5O_{12}]$ ($X = Fe^{2+}$, Co, Zn) and $Rb^2[XSi^5O^{12}]$ (X = Mn) leucites: comparison of monoclinic P21/c and Ia-3d polymorph structures and inverse relationship between tetrahedral cation (T = Si and X)—O bond distances and intertetrahedral T–O–T angles." *Acta Crystallogr. Sect. B: Struct. Sci.*, **74**(3), 274 (2018).
27. L. Bindi, A. M. Dymshits, A. V. Bobrov, K. D. Litasov, A. F. Shatskiy, E. Ohtani, and Y. A. Litvin, "Crystal chemistry of sodium in the Earth's interior: The structure of $Na_2MgSi_5O_{12}$ synthesized at 17.5 GPa and 1700°C." *Am. Mineral.*, **96**(2–3), 447 (2011).
28. A. M. T. Bell, C. M. B. Henderson, S. A. T. Redfern, R. J. Cernik, P. E. Champness, A. N. Fitch, and S. C. Kohn, "Structures of synthetic $K_2MgSi_5O_{12}$ leucites by integrated X-ray powder diffraction, electron diffraction and ^{29}Si MAS NMR methods." *Acta Crystallogr. Sect. B: Struct. Sci.*, **B50**, 31 (1994).
29. D. Wei, F. Du, Y. Huang, and H. J. Seo, "A novel green-emitting phosphor of Eu^{2+}-doped $Cs_2MgSi_5O_{12}$." *Mater. Lett.*, **65**(17), 2711 (2011).
30. J. C. de Mello, H. F. Wittmann, and R. H. Friend, "An improved experimental determination of external photoluminescence quantum efficiency." *Adv. Mater.*, **9**(3), 230 (1997).
31. F. Mazzi, E. Galli, and G. Gottardi, "The crystal structure of tetragonal leucite." *Am. Mineral.*, **61**(1-2), 108 (1976).
32. I. Yanase, H. Kobayashi, Y. Shibasaki, and T. Mitamura, "Tetragonal-to-cubic structural phase transition in pollucite by low-temperature X-ray powder diffraction." *J. Am. Ceram. Soc.*, **80**(10), 2693 (1997).
33. W. Zhang, D. Wei, and H. Jin Seo, "Eu^{2+}-doped pollucite $CsAlSi_2O_6$ with High luminescence efficiency for UV-pumped light-emitting diodes." *Mater. Lett.*, **94**, 140 (2013).

34. M. Zhang, Z. Xia, and Q. Liu, "Thermally stable $K_xCs_{1-x}AlSi_2O_6:Eu^{2+}$ phosphors and their photoluminescence tuning." *J. Mater. Chem. C*, **5**(30), 7489 (2017).
35. R. D. Shannon and C. T. Prewitt, "Effective ionic radii in oxides and fluorides." *Acta Crystallogr. Sect. B: Struct. Sci.*, **25**(5), 925 (1969).
36. A. M. T. Bell and C. M. B. Henderson, "Crystal structures and cation ordering in $Cs_2MgSi_5O_{12}$, $Rb_2MgSi_5O_{12}$ and $Cs_2ZnSi_5O_{12}$ leucites." *Acta Crystallogr. Sect. B: Struct. Sci.* (2009).
37. G. Blasse, "Energy transfer in oxidic phosphors." *Phys. Lett. A*, **28**(6), 444 (1968).
38. A. J. De Vries, H. S. Kiliaan, and G. Blasse, "An investigation of energy migration in luminescent diluted Gd^{3+} systems." *J. Solid State Chem.*, **65**(2), 190 (1986).
39. K. Vanheusden, C. H. Seager, W. L. Warren, D. R. Tallant, J. Caruso, M. J. Hampden-Smith, and T. T. Kodas, "Green photoluminescence efficiency and free-carrier density in ZnO phosphor powders prepared by spray pyrolysis." *J. Lumin.*, **75**(1), 11 (1997).
40. S. E. Brinkley, N. Pfaff, K. A. Denault, Z. Zhang, H. T. J. M. Hintzen, R. Seshadri, S. Nakamura, and S. P. DenBaars, "Robust thermal performance of $Sr_2Si_5N_8:Eu^{2+}$: An efficient red emitting phosphor for light emitting diode based white lighting." *Appl. Phys. Lett.*, **99**(24), 241106 (2011).
41. U.S. Department of Energy: Washington, D., U.S. Department of Energy, Office of Energy Efficiency and Renewable Energy. *Solid-State Lighting R&D Plan*, 2016.
42. J. McKittrick and L. E. Shea-Rohwer, "Review: Down Conversion Materials for Solid-State Lighting." *J. Am. Ceram. Soc.*, **97**(5), 1327 (2014).